FAST BEAD DETECTION AND INEXACT MICROARRAY PATTERN MATCHING FOR IN-SITU ENCODED BEAD-BASED ARRAY

Soumita Ghosh[1], Andreas Schmidt[1] and Dieter Trau[2]
[1]*AyoxxA Living Health Technologies, Singapore, Singapore*
[2]*Department of Bioengineering and Department of Chemical & Biomolecular Engineering,*
National University of Singapore, Singapore, Singapore

Keywords: Fast Inexact Graph Matching, Microarray Bead Detection, In-situ Encoded Bead-based Array, Graph Spectra, Sequence Alignment.

Abstract: This paper presents an automatic bead detection and bead array pattern matching technique developed for the In-situ Encoded Bead-based Array (IEBA) technology. A supervised learning based bead detection technique robust to irregular illumination variations and noise is developed. An efficient and effective graph matching technique that combines graph spectral analysis and sequence alignment is used to match bead array patterns. The matching algorithm proposed is rotation and scale-invariant. The pattern matching algorithm performs in-exact matching and is capable of handling very large numbers of outliers in the target graph as well as large number of occlusions in the template graph. The matching algorithm uses dynamic programming and can give good time performances dependent only on the number of nodes in the template and target graphs, irrespective of the number of outliers and occlusions. The algorithm can detect and match large number of beads in a few seconds.

1 INTRODUCTION

With the rapid progress of life sciences in the last decade various protein and DNA microarray formats have emerged. All these technologies have the common goal of detecting and measuring multiple biological markers in the same sample - so called ”multiplexing”. They have become the preferred choice when addressing complex questions in biomedical research as well as when screening clinical blood samples for multiple infectious disease or cancer markers at the same time in the same test. The latest generation of these ”biochips” include microscopic beads immobilized on silicon chips. These beads are coated with different biological agents like DNA-sequences or antibodies that can each detect a distinct marker. The central problem that remains is how to identify which microscopic bead is measuring which analyte? So far all commercial techniques use some kind of physical label to identify the beads. To provide an effective solution to multiplexing problem companies around the world offer beads either in different shades or colors or sizes or with tiny ”bar codes”. These approaches however make the process very tedious and require expensive and bulky equipments such as flow cytometers. Further using any kind of identifier limits the multiplexing capacity. For example, if color is used as the identifying marker then the multiplexing capacity is limited by the available color labels that can be robustly distinguished from each other.

In (Trau et al., 2008) the In-situ Encoded Bead-based Array (IEBA) technology was introduced to resolve the multiplexing issue in an effective way. The IEBA technology identifies randomly distributed beads on the biochip by obtaining the unique ”postal code” of each bead without use of any other marker on the beads. The postal code of each bead is the unique spatial address of each bead. In this paper we devise an algorithm using computer vision techniques to detect the beads and identify them without the use of any markers. Using such a marker less method a higher multiplexing capacity ($>$1000) can be achieved. The technique is developed using Ayoxxa Prokemion biochips. The chips contain multiple wells, with each well comprising of a complete multiplex microarray. The detection of analytes on the chip is based on a fluorescent signal. The quantitative fluorescent signal can be obtained using a fluorescent microscope, which is one of the most common equipment in any research laboratory. Additionally various high resolution fluorescent readers including automated high throughput screening lines used in in-

Ghosh S., Schmidt A. and Trau D..
FAST BEAD DETECTION AND INEXACT MICROARRAY PATTERN MATCHING FOR IN-SITU ENCODED BEAD-BASED ARRAY.
DOI: 10.5220/0003826800050014
In *Proceedings of the International Conference on Computer Vision Theory and Applications* (VISAPP-2012), pages 5-14
ISBN: 978-989-8565-04-4

dustry can be used to generate the fluorescence picture files as test read-out. To simplify the whole process we use a single fluorescent wavelength as a reporter for all analytes and all positive controls.

The analysis process involves finding correspondence between two different kinds of images which we call the manufacturing and fluorescent images. The set of images acquired after each batch of bead deposition during chip manufacturing are the manufacturing images and the set of images acquired after multiplex protein assay are called the fluorescent images. The measurement and protein quantification and analysis is carried out on these set of images. The fluorescent picture shows the beads after reacting with the different markers in the biological sample. The beads light up, with their intensity of fluorescence being directly proportional to the concentration of a certain analyte. It then remains to uncover the identity of the bead and find the biomarker it corresponds to.

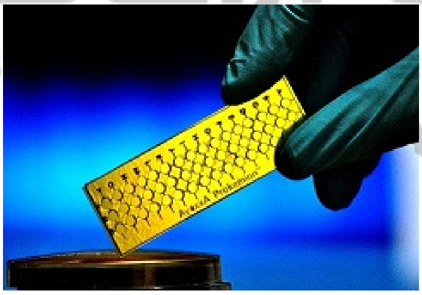

Figure 1: The Ayoxxa Prokemion biochip. The chip has a grid of circular wells. Each well is used for a sample.

The analysis process involves the following steps: detecting the beads in the manufacturing and fluorescent images, tracing the region of the manufacturing images that contains the fluorescent images and obtaining quantifiable measures like intensity and other parameters from the fluorescent image to determine the biomolecule that was attached to each individual bead. The software developed fully automates this analysis process. It uses two separate modules; one for detection of the beads and the other for matching between manufacturing and fluorescent beads. The detection is done using a supervised learning technique while the matching uses spectral properties of nearest-neighbour graphs and sequence matching algorithms.

In order for the software to be commercially viable both the detection and matching algorithms have to be very accurate and efficient. Furthermore, the algorithms have to be very robust to noise and other external factors. In particular for fluorescent images, since the environment under which they are captured cannot be controlled the images produced may vary in quality. Even slight variations in conditions may affect the quality by a large amount. Some of the common challenges involved in developing practical bead detection algorithms are handling image noise and irregular illumination. These can be caused by the human involvement in the imaging process and the imaging device setup. Further the microarray multiplexing technique is also not exact. Contaminations, dust and excess solution sticking to the surface can introduces impurities and make matching difficult. The main contributions of this paper are firstly the development of a practical and commercially viable bead detection algorithm for the IEBA technology that can detect beads of varying intensities and sizes under heavy noise and non-uniform illumination and secondly the development of a fast graph matching algorithm that can handle large mismatches and occlusions in the graphs.

Once a match for the fluorescent image is found in the manufacturing image, we also need to identify those manufacturing beads which are present within the matching region but do not have a corresponding match in the fluorescent image. This is used to extract information about the beads which were not captured under fluorescence but were present on the chip surface.

Section 2 gives a brief overview of the existing commercially used bead detection techniques and the available state-of-the-art pattern matching techniques. In Section 3 we present the bead detection techniques developed for identifying beads in the manufacturing and fluorescent images. Then in Section 4 we present the bead pattern matching technique. In Section 5 we present some performance results and in Sections 6 and 7 we draw conclusions and outline future improvements.

2 PREVIOUS WORKS

The most widely encountered problem in bead detection algorithms is that of irregular illumination. The manufacturing images often have irregular illumination due to reflection from within the imaging environment, due to external lighting or due to lens distortion. Insufficient drying of the chip surface before capturing images can also causes solution droplets to stick onto the surface and obstruct the bead pattern layout beneath it, resulting in loss of valuable information. Also, dust particles can get very heavily illuminated causing nearby beads to be brighter than usual. Figure 3 shows an irregularly illuminated manufacturing image where the beads near the centre of the well are well focused and are brighter than

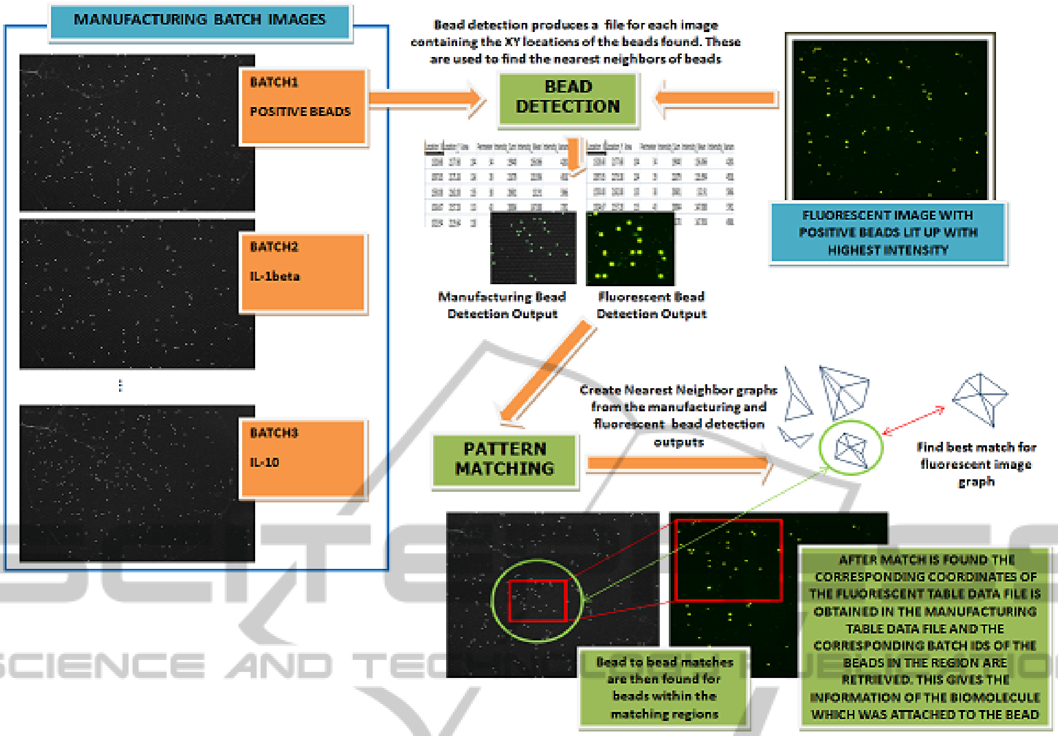
MANUFACTURING BATCH IMAGES
BATCH1
POSITIVE BEADS
BATCH2
IL-1beta
BATCH3
IL-10
Bead detection produces a file for each image containing the XY locations of the beads found. These are used to find the nearest neighbors of beads
BEAD DETECTION
FLUORESCENT IMAGE WITH POSITIVE BEADS LIT UP WITH HIGHEST INTENSITY
Manufacturing Bead Detection Output
Fluorescent Bead Detection Output
Create Nearest Neighbor graphs from the manufacturing and fluorescent bead detection outputs
PATTERN MATCHING
Find best match for fluorescent image graph
Bead to bead matches are then found for beads within the matching regions
AFTER MATCH IS FOUND THE CORRESPONDING COORDINATES OF THE FLUORESCENT TABLE DATA FILE IS OBTAINED IN THE MANUFACTURING TABLE DATA FILE AND THE CORRESPONDING BATCH IDS OF THE BEADS IN THE REGION ARE RETRIEVED. THIS GIVES THE INFORMATION OF THE BIOMOLECULE WHICH WAS ATTACHED TO THE BEAD

Figure 2: Illustrates the working of the system.

the ones near the edge of the well. Most commercially used automatic bead detection algorithms do not have to deal with such irregular illumination as most of the bio chip techniques use complex imaging devices that produce very high quality images. Further, besides using high quality image capturing systems most other techniques also use expensive readers to decode each bead uniquely. Some of the algorithms that do handle such irregular illumination need an additional pre-processing step to correct the image. Other techniques such as (Oliveros and Sotaquirà, 2007) use grids to simplify the detection process but require pre-processing to handle rotation. Our bead detection technique on the other hand does not use any global parameters and performs bead detection locally for each bead. Consequently the technique is inherently rotation and scale invariant and very robust against illumination variations and noise. Further to allow for robust bead detection we use two different kind of supervised learning techniques for the manufacturing and fluorescent images.

The main challenge in matching the fluorescent image with the manufacturing image is that the scale and orientation of the fluorescent image is unknown. Therefore a scale and rotation invariant matching technique is needed. Further since the bead detection algorithm cannot guarantee 100% accuracy there is always the possibility of a few beads missing or a few additional beads belonging to other batches being detected. Also as mentioned previously there is always the possibility of additional bead like structures being present in the manufacturing images due to contamination or dust. Therefore an exact matching is inadequate for the problem. Most computationally tractable point pattern matching algorithms assume that either the template or the query set does not have any noise. However in our case both the manufacturing and fluorescent image will have beads that are not present in the other. Fig. 2 shows an example of the bead detection and pattern matching process.

We formulate the problem of matching patterns of beads as a graph matching problem. The problem can be formally described as that of identifying the largest common isometric subgraph that best matches the template graph G (the manufacturing image bead pattern) in the query graph G' (the fluorescent image bead pattern).The problem of graph matching is a quadratic assignment problem and is NP-hard. The focus of graph matching research is therefore to effectively approximate the exact solution. In a recent work (J.McAuley and S.Caetano, 2012) developed a matching algorithm that gives good empirically formulated results under noise. The algorithm however has a major drawback. The complexity of the algorithm is dependent on the number of missing beads in the template graph. In our problem matching has to

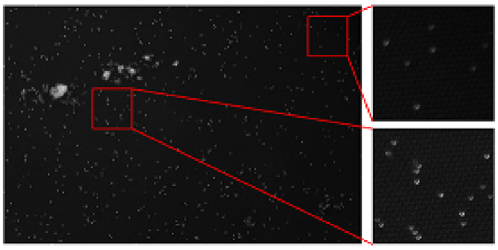

Figure 3: Shows an irregularly illuminated manufacturing image. The beads close to the top right corner are less bright due to lens distortion while the beads close to the noise are brighter than the average beads because of the high luminance of the dust particles.

work even when as much as 25% of the beads in the fluorescent image are missing.

Further the manufacturing image has thousands of beads and an exhaustive search for scale and rotation invariant match is impractical. Most fast graph matching algorithms either performs only exact matching or make too many assumptions (H.Alt and L.J.Guibas, 1996) and (Rezende and Lee, 1995). To perform inexact matching and still keep the time performance reasonable we take a two step approach. First we use a fast graph spectra based technique to identify regions in the manufacturing image that are likely to have a match for the beads in the fluorescent image. We then use a more demanding sequence matching technique to identify the most optimal bead to bead matches between manufacturing and fluorescent beads as well as identify beads in each image which are missing in the other.

Graph spectra is used to identify beads in the manufacturing image which are similar to the beads in the fluorescent image. Since the development of spectral matching in (Leordeanu and Heberti, 2005) numerous other graph spectra based graph matching techniques such as (Cour et al., 2006) have been developed. These techniques use the graph spectra of an assignment graph whose nodes represent potential matches between the template graph (G) and query graph (G') nodes and whose edge weights represent the potential agreement between match pairs. The Eigenvalue decomposition of the assignment graph has a time complexity of $O(|G|^3|G'|^3)$. This prohibitively high time complexity restricts the use of spectral techniques to matching smaller graphs. We avoid this problem by using graph spectra only as a local descriptor.

The estimation of the location of a bead in both the fluorescent and the manufacturing images can have some errors and therefore an error tolerant matching is necessary. We use the tolerance estimation technique used in (Evans and Tay, 1995) to estimate the tolerance values for each spectral feature individually from a training dataset.

The Smith-Waterman algorithm (Smith and Waterman, 1981) is used in the second step to find the most optimal set of bead to bead matches. The Smith-Waterman algorithm was originally developed for finding common molecular subsequence and therefore has to be modified slightly for use in our matching problem. The algorithm is implemented using dynamic programming and has a complexity of $O(mn)$ where the sequences to be matched are of length m and n. Smith-Waterman algorithm has also been used previously for shape matching in (Chen et al., 2008) and (Riedel et al., 2006). It has the nice property that it produces the optimal local alignment with respect to the scoring system.

3 BEAD DETECTION

3.1 Manufacturing Bead Detection

In order to overcome the irregular illumination problem we use a local adaptive thresholding technique. The thresholding is performed by calculating the intensity distribution of small square patches in the image and thresholding out the highest 5% of the intensities. A sliding window with no overlap is used to threshold the entire image. The size of the patches is about 10 times the normal diameter of beads. This allows a very optimistic thresholding i.e. it tries to identify beads everywhere. Even for large illuminated areas the algorithm extracts only the brightest regions. The normal diameter of beads is learnt from the radius feature described later and the 5% cut-off is estimated empirically. Contour detection is then applied on the binary images using algorithm developed by (S.Suzuki and K.Abe, 1985). The regions of the manufacturing image fully enclosed by each closed contour are then extracted. The maximum intensity and mean location (mean x and y coordinates) of each region is calculated. The locations are then used as seeds for region growing while the maximum intensities are used to estimate the intensity threshold to stop the region growing.

Small amount of region dilation is then performed for each region using a circular structuring element of radius 3 pixels to make the edges smooth.

Following this for each region the following set of shape, size and intensity features are extracted: Area, Perimeter, Intensity Sum, Intensity Mean, Intensity Variance, Minimum Intensity, Maximum Intensity, Radius Mean, Radius Variance, Minimum Radius, Maximum Radius and Orientation. Where the area and perimeter features are the number of pixels inside the region and on the contour respectively. The area and perimeter features deal with both size and shape of the feature. For e.g. a very large perimeter for a small area is indicative of a rough contour or a concave region. The Intensity Sum, Intensity Mean, Intensity Variance, Minimum Intensity, Maximum Intensity features deal with the intensity distribution of the region. The sum of intensities and mean are indicative of the overall brightness of the region. The intensity variance and minimum and maximum intensities are indicative of the overall change in intensity from the centre of the region to the edge of the region. A very high variance in intensity or a large maximum intensity to minimum intensity ratio is indicative of an unevenly bright spot. The radius mean, radius variance, minimum radius, maximum radius are calculated as the mean, variance, minimum and maximum respectively of the distances from the centre of the region to each contour pixel. The Radius mean and radius variance features also deal with the overall shape of the region. True beads tend to show a slightly oval shape and therefore have a moderate radius variance and a rather stable minimum to maximum radius ratio. For any particular manufacturing image, beads are also found to be oriented in the same way. The orientation feature is used to encapsulate this property. It is calculated as the angle the longest axis of the region makes with the y-axis.

A binary one-to-one support vector machine is then trained using the above 12 features to classify the extracted regions as bead and non-bead regions. Classification results are presented in Section 5.

3.2 Fluorescent Bead Detection

The same set of features as the ones extracted for detecting manufacturing beads are also extracted for fluorescent bead detection. However for the final classification instead of using a single support vector machine a number of support vector machine classifiers are trained. This is necessary because beads of different batches in the manufacturing process differ heavily in appearance in both size and intensity. Further estimating the batch of the bead directly from the intensity becomes a multi-class classification problem which can significantly reduce the accuracy, even when classification is done by max-wins voting strategy. For our particular problem we found that training a single one-versus-all support vector machine classifier for each batch gave the best results.

4 BEAD PATTERN MATCHING

Once the bead patterns and their respective batches have been estimated the relative locations of beads is used to find matches. For a particular batch the intensity, shape, size and orientation of all beads are very similar and therefore these features cannot be used to distinguish between them. The only feature that distinguishes a bead is the relative position of other beads with respect to that bead. That is the pattern formed by the neighbours of a bead is the identifier of the bead.

The bead matching is done in two steps. In the first step the graph spectra of the fully connected weighted graph formed using the bead and its 3 nearest neighbours is used to find a region of the manufacturing image that is most likely to have a matching pattern. The spectrum of the affinity matrix of a graph has the nice property of being invariant to rotation and labelling. This allows the first step of the matching to be rotation invariant. Further using the normalized Laplacian of the graph instead of the adjacency matrix makes the matching invariant to scale. The edge weights are simply the Euclidean distance between the bead centres. The graph spectra is calculated by doing an Eigen value decomposition of the normalized graph Laplacian. The graph Laplacian is calculated as follows:

$$L(u,v) = \begin{cases} 1, & \text{if } u = v \\ \frac{-w(u,v)}{\sqrt{d_u d_v}}, & \text{if } u \text{ and } v \text{ are adjacent} \\ 0, & \text{otherwise} \end{cases} \tag{1}$$

where

$$d_u = \sum_v w(u,v) \tag{2}$$

and $w(u,v)$ is the weight of the edge between nodes u and v.

The choice of the number of nearest neighbours depends on the amount of mismatch in the graphs. For our implementation the value of 3 was chosen empirically. Using 3 nearest neighbours means that in order to find a correct match there should be at least one bead in the fluorescent image for which its 3 nearest neighbour pattern matches the 3 nearest neighbour pattern of its true corresponding bead in the manufacturing image. This is a reasonable assumption particularly for dense patterns. In case of sparse patterns using even 2 nearest neighbours produced good results. Using a small number of nearest neighbours is necessary because in this step we intend to find matches which are very similar to each other. In particular we try to find matches where nodes are not missing and differences in the two graphs are only because of error in determining the location of the beads during the detection process. This step however provides many possible matches and is used to locate the regions of the manufacturing image that is likely to have the matching pattern. Further the matching is extremely fast because of the small size of the graph Laplacian. The Eigen decomposition of the 4x4 graph Laplacian gives 4 Eigen values. The first Eigen values deals with the scale of the graph and since we are interested in a scale invariant match it is ignored. The remaining 3 Eigen values are used to find the matches. Matching the 3-tuple graph spectra of two graphs is done using a tolerance value for each dimension. The tolerance value for each dimension is calculated as the standard deviation of that dimension for true matches and is estimated using a training dataset.

The graph spectra based matching produces a set of possible matches in the manufacturing image for each fluorescent bead. These possible matches are then further refined in the second step using a larger set of nearest neighbours and a sequence matching technique. The nearest neighbours of a bead in this step are defined as a set of distance-angle pairs instead of just distances. The angle for the kth nearest neighbour is calculated as the angle formed between the line connecting the bead to its first nearest neighbour and the line connecting the bead to its kth nearest neighbour. This allows the matching to be rotation invariant. In order to make the matching scale invariant the distances are normalised by dividing all distances by the distance to the first nearest neighbour. The sequences are finally formed by sorting the distance-angle pairs first by distance and then by angle.

A slightly modified version of the Smith-Waterman sequence alignment algorithm is used to find the match between nearest neighbour sequences for each fluorescent-manufacturing bead match found in the first step. Instead of doing exact matches of characters as in the original Smith-Waterman algorithm an error tolerant matching of distance-angle pairs is used where some tolerance is allowed for both the distance and angle values. In this case however the effect of tolerance is much less significant because of the use of both the angle and distance. The score matrix for two sequences a and b of lengths m and n respectively is defined as:

$$H(i,j) = \begin{cases} 0, & \text{if } i=0 \text{ or } j=0 \\ max \begin{cases} 0, \\ H(i-1,j-1)+w(a_i,b_i), \\ H(i-1,j)+w(a_i,-), \\ H(i,j-1)+w(-,b_i) \end{cases} & \text{else} \end{cases} \qquad (3)$$

where

$$w(a_i,b_i) = \begin{cases} match\_score, & \text{if } a_i = b_i, \\ mismatch\_score, & \text{otherwise} \end{cases} \qquad (4)$$

and

$$w(a_i,-) = w(-,b_i) = gap\_score \qquad (5)$$

The values for *gap_score*, *match_score* and *mismatch_score* were empirically found to be -9.0, 10.0 and -8.0 respectively. The Smith-Waterman algorithm however does not guarantee an exact match for each element of the sequences. For instances for two sequences of distance-angle pairs shown in table 1 below:

Table 1: Example sequence.

A	119,7.47	166,7.19	321,5.22	60,4.98
B	127,7.59	166,7.23	35,6.13	60,5.01

Smith-Waterman algorithm can produce an alignment as shown below:

Table 2: Example sequence alignment.

119,7.47	-
-	127,7.59
166,7.19	166,7.23
321,5.22	**35,6.13**
60,4.98	60,5.01

Since we are interested only in finding exact bead to bead matches an additional correction step is needed which identifies mismatches in the aligned sequences such as the one in the 4th row of table 2 and changes the sequence alignment to correct them.

The best matching fluorescent and manufacturing bead pair is identified as the one that gives the highest percentage of matching distance-angle pairs. In case more than one fluorescent and manufacturing bead pair produces the same percentage of distance-angle pair matches, the one with the smallest sum of squared error is defined as the best match. The sequence matching directly gives the bead to bead matches for all fluorescent image beads as well as gives the manufacturing and fluorescent beads for which matches were not found.

Finally, the scale and rotation of the matching pattern are estimated as the modes in the ratio of distances and the difference of angles between the fluorescent and its corresponding manufacturing bead. Once the scale and rotation angle have been estimated the missing fluorescent beads are located by back tracking their location in the manufacturing image.

5 RESULTS

Testing was performed on a set of manually labelled manufacturing and fluorescent images. For testing detection performance artefacts in both manufacturing and fluorescent images were manually labelled as beads and non-bead artefacts. For quantifying the pattern matching performances the most optimal match for each fluorescent image's bead pattern was manually found in a set of manufacturing images and the exact bead to bead matches were also manually found.

To evaluate the performance of the detection algorithm the specificity, sensitivity, precision and accuracy of detection were used.

For testing detection accuracy on fluorescent images bead detection was performed on a set of 40 fluorescent images acquired under different experimental conditions over a long period of time. Table 3 shows the detection results for a 10-fold cross validation on fluorescent beads. For fluorescent images the detection algorithm shows high accuracy and precision and as well as high specificity and sensitivity.

Table 3: 10-fold cross validation results of detection on a set of 40 fluorescent images.

Performance Measure	Mean	Standard Deviation
Sensitivity	0.974	0.016
Specificity	0.988	0.015
Accuracy	0.980	0.003
Precision	0.993	0.009

Bead detection was also evaluated on 20 manufacturing images. The images were acquired under a large range of conditions and the dataset was designed to have images with large variations in noise levels as well as irregular illumination levels. Typically manufacturing images have a very large number of beads (>500) and therefore manually identifying all positive and negative beads is extremely tedious. The data set used here for example contained over 10000 beads. Therefore to generate the labelled data a semi-supervised technique was used. A naive Bayes classifier was trained to classify the most obvious beads as true beads. This classifier was trained very conservatively and therefore high confidence could be put on its positive results. In essence whenever the classifier found even slight variations in the features with respect to the features of the positive class it classified the bead as negative. An interface was also developed that allowed the program to sequentially present beads identified by the naive Bayes classifier as negative to the user for manual classification.

Table 4 shows the performance results for manufacturing bead detection. The algorithm achieves high specificity and sensitivity as well as high accuracy and precision even for manufacturing images. The sensitivity in the case of manufacturing image is however slightly lower than that of fluorescent images as the percentage of actual beads to the total number of artefacts in the image is much smaller and this bias increases the number of false negatives.

Table 4: 10-fold cross validation results of detection on a set of 20 manufacturing images.

Performance Measure	Mean	Standard Deviation
Sensitivity	0.919	0.019
Specificity	0.997	0.003
Accuracy	0.973	0.006
Precision	0.993	0.008

To test the robustness of the algorithm against noise simulated noisy manufacturing images were generated by adding Salt and Pepper noise to the original images. Adding salt and pepper noise has two effects, first it arbitrarily changes the shapes of the true beads and second when large amount of noise is added, artificial artefacts similar to real noise patterns caused by dust particles are formed. Figure 4(a) shows a section of a manufacturing image and figure 4(b) shows the same section with 10% noise added to it. Detection was performed on a set of 5 manufacturing images with each image having 6 instances with different levels of noise added. Figure 5 shows the detection performance on the set of images with respect to different levels of noise. The detection algorithm shows good resistance against noise and is able to handle noise as high as 10%.

To test detection performance against irregular illumination synthetic manufacturing images were created from the original images by adding a grayscale gradient map. Figure 6(a) shows an original manufacturing image and figure 6(b) shows the synthetic image constructed by adding a gradient map with mean intensity of 128 and 50% opacity to the original image. Figure 7 shows the detection performance against different levels of irregular illumination. As can be seen both form the detection output in figure 6(b) and in figure 7 the algorithm is capable of handling very large amount of illumination variations. The number of false positives starts to increase sharply at 40% opacity while at the same time the number of false negatives reduces significantly as more and more artefacts in the image are extracted and classified. This effect can be seen in figure 7 where the specificity starts to increase as opacity is increased beyond 40%.

Pattern matching performance is evaluated on 5 sets of 3 manufacturing and 3 fluorescent images. For each fluorescent image a match is found in one of the three manufacturing images giving a total of 15 pattern matches. Together the 15 fluorescent images contain over 700 beads for which bead to bead matches were detected. The fluorescent bead patterns to be matched vary heavily in bead density and in the number of beads within the pattern actually having a match in the manufacturing image. The true

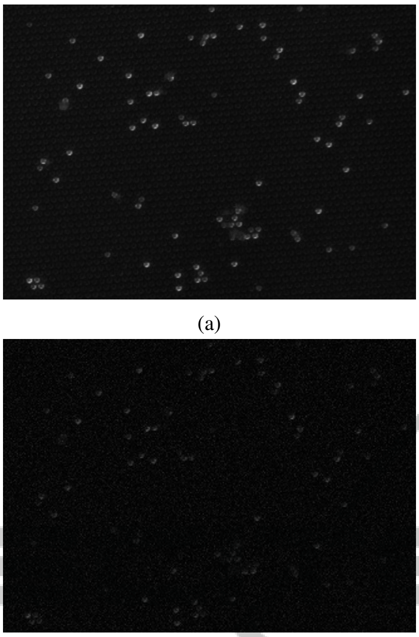

(a)

(b)

Figure 4: (a) shows the original section of a manufacturing image and (b) shows the same section with 10% salt and pepper noise. Here 10% noise means 10% of the pixels have been randomly set to the mean intensity of beads.

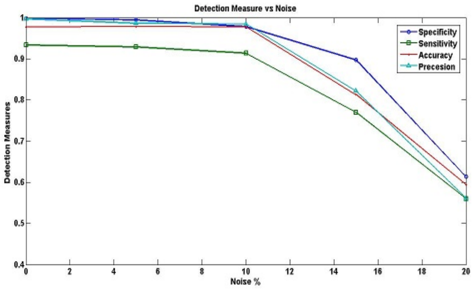

Figure 5: Shows the change in Specificity, Sensitivity, Accuracy and Precision with changing noise levels.

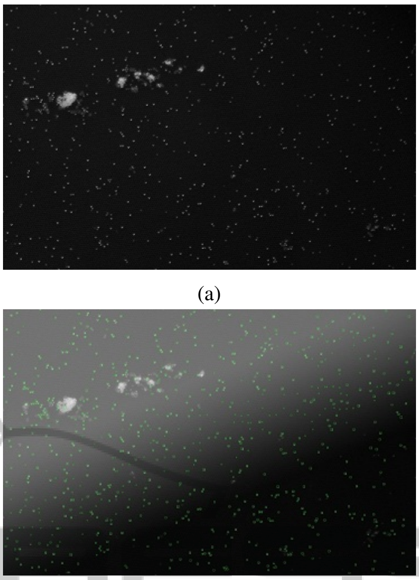

(a)

(b)

Figure 6: (a) shows the original manufacturing image and (b) shows the bead detection output on the same image with 50% gradient. Here 50% gradient means a gradient map with mean intensity of 128 and 50% opacity has been applied to the original image. The detection algorithm output is evenly distributed irrespective of the illumination level. However, at this level of irregularity the false positive rate of detection starts to increase sharply.

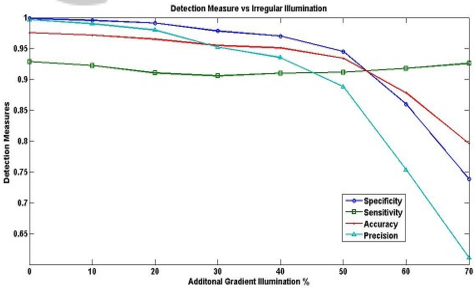

Figure 7: Shows the change in Specificity, Sensitivity, Accuracy and Precision with changing levels of irregular illumination.

positives in this case are identified as correct bead to bead matches for all beads within the bounding region of the matching patterns (for fluorescent image this means the entire image). This includes predicted matches for manufacturing beads not present in the fluorescent image that is beads that did not react or were not detected. True negatives are those beads in the fluorescent image which are missing in the manufacturing image and for which a match was not found. These are the beads that were activated because of contamination. False positives are incorrectly identified bead to bead matches while false negatives are fluorescent image beads which do not have a true match in the manufacturing image but a match was detected. Once again we use specificity, sensitivity, precision and accuracy to evaluate the matching performance. Table 5 shows the results for the 15 matches.

Table 5: Bead to bead matching results for 15 fluorescent image patterns.

Performance Measure	Mean	Standard Deviation
Sensitivity	0.382	0.185
Specificity	0.988	0.010
Accuracy	0.923	0.021
Precision	0.931	0.022

The results show good sensitivity, accuracy and precision but a strikingly low specificity. This is because of a large bias towards the positive class. Typically most fluorescent beads have a true match in the manufacturing image and only very few beads in the fluorescent image are those which reacted and brightened up due to contamination. Therefore although the Precision is high the number of false positives is comparable to the number of true negatives and false negatives.

Fluorescent images of higher batches tend to have very high bead densities and a larger mismatch can be found between the fluorescent image beads and the actual matching manufacturing beads. Beads that lit up due contamination and beads that did not react or were not detected can together cause the true matching regions in the two images to have less than 30% of the matching beads. Matching under such heavy occlusion conditions and with outliers is one of the strengths of this algorithm. To evaluate the matching performance under such conditions simulated data is created by adding and removing beads to the fluorescent images and to the region of the manufacturing image containing the true match. The results of testing on a set of 15 fluorescent manufacturing image pairs is shown in figure 8. The amount of mismatch is quantified as the ratio of synthetic beads added and original beads removed to the number of total matching beads.

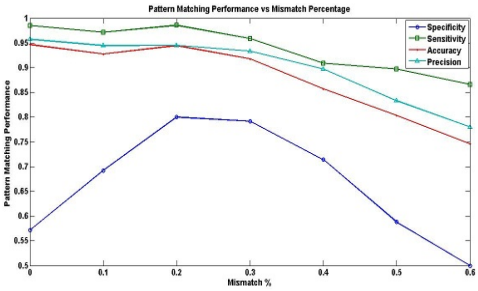

Figure 8: Shows the change in Specificity, Sensitivity, Accuracy and Precision with changing levels of mismatch between the fluorescent bead pattern and the manufacturing bead pattern. Here the amount of mismatch is quantified as the ratio of the sum of synthetic beads added to the fluorescent image and manufacturing beads removed to the number of total manufacturing beads with true bead to bead match in the fluorescent image.

Similar to the results in table 3 the specificity is low in figure 8 as well. However as the amount of mismatch increases initially the specificity also increases as more instances of the negative class are added to the data and therefore the bias towards the positive class decreases. However after a certain level of mismatch all the performance measures start declining sharply. This is due to the cases where overall matching fails all together. The matching algorithm requires at least one bead with similar 3-NN structure in both the fluorescent and manufacturing image. As the mismatch exceeds 30% this is not satisfied in some cases. Similarly even at very high mismatches such as 60% in some cases true matches are found. In general however when the 3-NN criterion is satisfied very high sensitivity, precision and accuracy are achieved.

Another major strength of this algorithm is that it is fast and scales well with increasing size of the graphs. State-of-the-art graph matching algorithms that can deal with occlusions and outliers have quadratic or quasi-quadratic complexity. Our algorithm on the other hand has almost linear complexity. The time performance of the algorithm was evaluated on a manufacturing data set with 6 images where each subsequent image had greater number of beads. Matching was performed for 5 fluorescent images with number of beads ranging from 70 to 80. Testing was done on a workstation with Pentium Core 2 duo 2.1 GHz processor with 2.0 GB RAM. Figure 9 shows that the time taken to match increases almost linearly with the number of beads in the manufacturing images. This is because most of the matching is done using graph spectra and calculating the spectra of a 4x4 matrix is extremely fast. The number of possible matches identified using graph spectra also does not increase rapidly with increasing number of nodes. When the number of beads range from 250 to 500, which is the most significant range for us the time taken to match is between 6 to 20 seconds.

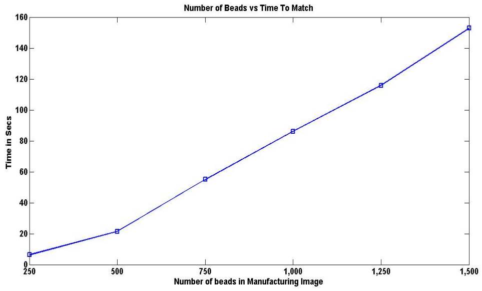

Figure 9: Shows the time taken to find a match with increasing graph sizes.

6 CONCLUSIONS

The future of the healthcare lies in 'Personalized Medicine' which tailors the medical treatment of an individual based on his/her profile characteristics (Priorities for Personalized Medicine, 2008). This is beneficial in many ways as treating all patients in the same way not only ignores the individual conditions and specific therapy requirements of each individual but also incurs excess cost to the healthcare system.

Improvement in healthcare system requires closer collaboration with technologies from multidisciplinary background. Use of advanced computer vision and machine learning techniques are of vital importance to resolve many issues in medical applications. In present days no technology can be isolated from the other in creation of a successful commercially viable product. The bead detection and pattern matching algorithm developed here specifically solves some of the problems such as handling noisy image data, irregular illumination and occlusion and outlier resistant pattern matching involved in the IEBA technology. The IEBA technology together with automated fast bead detection and inexact microarray pattern matching effectively uses computer vision and machine learning algorithms and promises to be an excellent platform for protein multiplexing and take medical diagnostics to the next level.

REFERENCES

Chen, L., Feris, R., and Turk, M. (2008). Efficient partial shape matching using smith-waterman algorithm. In *In CVPR workshop on Non-Rigid Shape Analysis and Deformable Image*.

Cour, T., Srinivasan, P., and Shi, J. (2006). Balanced graph matching. In *NIPS*.

Evans, D. J. and Tay, L. P. (1995). Fast learning artificial neural networks for continuous input applications. In *Kybernetes*.

H.Alt and L.J.Guibas (1996). Discrete geometric shapes:matching,interpolation,and approximation: A survey. In *Technical Report, Handbook of Computational Geometry*.

J.McAuley, J. and S.Caetano, T. (2012). Fast matching of large point sets under occlusions. In *Pattern Recognition 45 (2012)*. Elsevier.

Leordeanu, M. and Heberti, M. (2005). A spectral technique for correspondence problems using pairwise constraints. In *ICCV*.

Ng, J. K., Selamat, E. S., and Liu, W.-T. (2008). A spatially addressable bead-based biosensor for simple and rapid dna detection. In *Biosensors & Bioelectronics*. Elsevier.

Oliveros, A. and Sotaquirà, M. (2007). An automatic gridding and contour based segmentation approach applied to dna microarray image analysis. In *International Journal of Biological and Life Sciences*.

Priorities for Personalized Medicine (2008). (PCAST 2008). Technical report, Presidents Council of Advisors on Science and Technology.

Rezende, P. and Lee, D. (1995). Point set pattern matching in d-dimensions. In *Algorithmica 13(1995)*.

Riedel, D. E., Venkatesh, S., and Liu, W. (2006). A smith-waterman local alignment approach for spatial activity recognition. In *In Proceedings of AVSS'2006*.

Smith, T. F. and Waterman, M. S. (1981). Identification of common molecular subsequences. In *Journal of Molecular Biology*.

S.Suzuki and K.Abe (1985). Topological structural analysis of digital binary image by border following. In *Computer Vision, Graphics, and Image Processing, Vol. 30, No. 1*.

Trau, D., Liu, W.-T., and Ng, J. K. K. (2008). A microarray system and a process for producing microarrays. In *International Publication Number WO 2008/016335 A1*.